

Article

PrBaCo₂O_{6−δ}-Ce_{0.8}Sm_{0.2}O_{1.9} Composite Cathodes for Intermediate-Temperature Solid Oxide Fuel Cells: Stability and Cation Interdiffusion

Dmitry Tsvetkov¹, Nadezhda Tsvetkova¹, Ivan Ivanov¹, Dmitry Malyshkin^{1,2}, Vladimir Sereda^{1,2} and Andrey Zuev^{1,*}

¹ Department of Physical and Inorganic Chemistry, Institute of Natural Sciences and Mathematics, Ural Federal University, Ekaterinburg 620000, Russia; Dmitry.Tsvetkov@urfu.ru (D.T.); Nadezhda.Tsvetkova@urfu.ru (N.T.); Ivan.Ivanov@urfu.ru (I.I.); Dmitry.Malyshkin@urfu.ru (D.M.); Vladimir.Sereda@urfu.ru (V.S.)

² Institute of High-Temperature Electrochemistry UB RAS, Ekaterinburg 620137, Russia

* Correspondence: Andrey.Zuev@urfu.ru

Received: 29 December 2018; Accepted: 23 January 2019; Published: 29 January 2019



Abstract: The single-phase oxide PrBaCo₂O_{6−δ} and composites (100 − *y*)PrBaCo₂O_{6−δ}-*y*Ce_{0.8}Sm_{0.2}O_{1.9} (*y* = 10–30 wt.%) were investigated as cathode materials for intermediate-temperature solid oxide fuel cells. The chemical compatibility, cation interdiffusion, thermal expansion and dc conductivity were studied. As a result, strong interdiffusion of Pr and Sm was found between PrBaCo₂O_{6−δ} and Ce_{0.8}Sm_{0.2}O_{1.9}. This leads to only insignificantly decreasing thermal expansion coefficient of composite with increasing fraction of Ce_{0.8}Sm_{0.2}O_{1.9} and, thus, mixing PrBaCo₂O_{6−δ} with Ce_{0.8}Sm_{0.2}O_{1.9} does not improve thermal expansion behavior of the cathode material. Moreover, formation of poorly-conducting BaCeO₃, caused by chemical interaction between the double perovskite and doped ceria, was shown to lead to pronounced drop in the electrical conductivity of the composite cathode material with increasing Ce_{0.8}Sm_{0.2}O_{1.9} content.

Keywords: double perovskite; solid oxide fuel cells; chemical compatibility; interdiffusion; electrical conductivity; thermal expansion

1. Introduction

Solid oxide fuel cells (SOFCs) have already attracted great attention in the last few decades as alternative power generation devices with high working efficiency and environmental safety. Operating temperature lowering is to be the general way to promote the commercial application of SOFCs because it broadens the range of compatible construction materials, prolongs their life-time and, as a consequence, reduces the cost of energy production.

The double perovskites RBaCo₂O_{6−δ} (where *R* is a rare-earth element) have been recently proposed as potential cathode materials for intermediate-temperature SOFCs (IT-SOFCs) because of their fast oxide ion transport, high mixed ionic and electronic conductivity as well as high catalytic activity with respect to the oxygen reduction [1–13]. PrBaCo₂O_{6−δ} (PBC) was shown to possess the most attractive properties [1,4,6–8,14–16] among the variety of cobaltites with double perovskite structure and, consequently, can be considered as one of the most promising cathode materials. Despite the numerous publications devoted to study of the properties of PBC, there are significant inconsistencies in the reported values of electrical conductivity and polarization resistance [4,6–8,14,17–21]. Indeed, the value of maximum conductivity of PBC in air was found by Zhao et al. [17] to be equal to 317 S·cm^{−1} as against 2000 S·cm^{−1} and 1343 S·cm^{−1} reported by Kim et al. [14] and Zhou et al. [18], respectively. It should be noted also that possible influence of solid

electrolyte material on the electrochemical performance of composite cathodes based on $R\text{BaCo}_2\text{O}_{6-\delta}$ ($R = \text{Pr, Nd, Sm, Gd}$) still remains a controversial topic. For example, the polarization resistance of the $\text{PrBaCo}_2\text{O}_{6-\delta}\text{-Ce}_{0.8}\text{Sm}_{0.2}\text{O}_{1.9}$ (PBC-SDC) cathodes was found [11,20] to decrease with increasing electrolyte content, whereas opposite trend was shown in Reference [18]. Moreover, the reported results on chemical compatibility between double perovskites and ceria-based electrolytes are also controversial [10–23]. Indeed, chemical interaction between ceria-based electrolytes and double perovskite cathodes was found in some works [10,22], while a good chemical compatibility between these materials is mostly claimed [11–23]. Unfortunately, the compatibility found is, most likely, a result of kinetic limitations because it seems to be inconsistent with the thermodynamics of the PBC-SDC mixture. Indeed, enthalpies (calculated on the basis of available thermodynamic data [24–29]) of the following chemical reactions:



and



are negative at 298 K and one can expect that they only weakly depend on temperature. Besides, aforementioned reactions seem to proceed without significant entropy change, since all the reactants are solid species. This allows expecting a negative change of Gibbs free energy in both reactions and, consequently, strong interaction between the mixture components.

As pointed out in Reference [22], investigation of chemical compatibility by heating a physical mixture of cathode and electrolyte powders at high temperature for several hours followed by analyzing of its phase composition using X-Ray diffraction (XRD) still remains the easiest and most common way to check whether a cathode material is compatible with selected electrolyte or not. In this way, presence of, at least, any third phase is interpreted as evidence of incompatibility, whereas absence of such phase is regarded as indication of full compatibility of the cathode and electrolyte materials. However, firstly, such judgment depends very much on annealing conditions, especially on its duration, because of the kinetic limitations of solid-state interaction. Secondly, oftentimes, no clear evidence of new phase formation or cation interdiffusion can be assessed on the basis of XRD analysis only, owing to the nonzero detection limits of conventional XRD [22].

In this respect, thermodynamic analysis of materials' compatibility is completely free from such limitations and, probably, represents the only way of unambiguous interpretation of compounds' stability under particular conditions. Therefore, it is of key importance (i) to carry out such analysis for PBC material in order to assess its behavior as cathode for ceria-based SOFCs in different atmospheres and then (ii) to understand the influence of possible chemical interactions on the PBC cathode electrochemical performance.

2. Materials and Methods

Powder samples of the double perovskite PBC and solid electrolyte $\text{Ce}_{0.8}\text{Sm}_{0.2}\text{O}_{1.9}$ (SDC) were prepared by means of glycerol-nitrate method described in detail elsewhere [24]. Pr_6O_{11} , BaCO_3 , Co , $\text{Ce}(\text{NO}_3)_4 \cdot 6\text{H}_2\text{O}$ and Sm_2O_3 were used as starting materials. All materials used had a purity of at least 99.9%. The final calcination of both PBC and SDC was carried out at 1100 °C in air.

The phase composition of powder samples prepared accordingly was investigated by means of X-ray diffraction with Equinox 3000 diffractometer (Inel, Artenay, France) using $\text{Cu K}\alpha$ radiation. The XRD showed no indication for the presence of a second phase in the as-prepared PBC and SDC.

The chemical composition of all the oxides under investigation was preliminary checked using ICP spectrometer ICAP 6500 DUO (Thermo Scientific, Waltham, MA, USA) and atomic absorption spectrometer Solar M6, Thermo Scientific, Waltham, MA, USA. All the samples used for measurements were shown to have the stoichiometric composition with respect to metal cations within the accuracy of 2%. No impurities were found within the same accuracy range as well.

Composite materials $(100 - y)\text{PBC}-y\text{SDC}$ were prepared by mechanical mixing of PBC and SDC powders in different weight ratios within the range of $y = 10\text{--}30$ wt.%. The powders of the double perovskite and electrolyte materials were thoroughly mixed in ethanol using agate mortar and pestle.

The chemical compatibility of PBC and SDC was studied by means of homogenizing annealing of 50:50 (wt.%) mixtures at different temperatures in the temperature range between 1000 and 1200 °C for 12 h in air followed by fast cooling and phase analysis (XRD) of products.

Cation interdiffusion between PBC and SDC was studied by means of annealing the diffusion couple. The PBC and SDC ceramic pellets used for interdiffusion experiments were prepared by uniaxial pressing the single-phase PBC and SDC powders at 20 MPa in disks 9 mm in diameter and 3 mm in height. The as-prepared green sample disks were then sintered in air at 1250 °C and 1500 °C in the case of PBC and SDC, respectively. Sintered ceramics with 90% relative density were then polished using diamond abrasive paste. The diffusion couple was prepared by spring-loading the polished ceramic pellets of PBC and SDC in a homebuilt sample holder. As-prepared diffusion couple was then annealed at 1000 °C for 30 h in air. After annealing, it was mounted into an epoxy resin, cut perpendicular to the PBC-SDC interface and polished with diamond abrasive paste. The cross-section of the as-prepared diffusion couple was studied by scanning electron microscopy (SEM) coupled with energy dispersive spectrometry (EDX) using an AURIGA CrossBeam (FIB-SEM) Workstation (Carl Zeiss SMT, Oberkochen, Germany).

Rectangular bars of $30 \times 3 \times 3$ mm³ for electrical conductivity and thermal expansion measurements were prepared by dry pressing at 20 MPa and sintering for 12 h in air at 1200 °C and 1300 °C for PBC (as well as for the composites) and SDC, respectively.

Thermal expansion of the samples prepared accordingly was measured using DIL 402C dilatometer (Netzsch GmbH, Selb, Germany) in the temperature range 30–1000 °C in air.

Electrical conductivity of the composite materials $(100 - y)\text{PBC}-y\text{SDC}$ and the single-phase double perovskite PBC was measured by means of 4-probe dc-method in the temperature range 500–1000 °C in air. The experimental setup and technique employed for the conductivity measurements are described in detail elsewhere [30].

3. Results and Discussion

3.1. Thermodynamic Analysis

As mentioned in the Introduction, even simple thermochemical considerations indicate instability of double perovskite PBC due to thermodynamic possibility of its chemical interaction with ceria-based electrolytes. Therefore, a general thermodynamic assessment of stability of the double perovskite under different conditions is strongly required to understand the behavior of PBC as a component of the SOFC cell. Such analysis was carried out in the two cases: (1) In the CO₂ atmosphere and (2) in contact with CeO₂ as the parent phase for the state-of-the-art intermediate-temperature solid electrolytes. However, one should emphasize that the exact thermodynamic analysis is nowadays impossible since thermodynamics of the Pr-Ba-Co-O system is poorly studied so far. It is noteworthy that there is lack of reliable data on standard thermodynamic functions of complex oxides in the system studied, except PrCoO₃ and PBC. The required information for PrCoO₃ was taken from References [27,28].

The standard formation enthalpy of PBC at 298 K was measured by us earlier [24] as a function of oxygen content. However, neither the standard entropy of PBC nor that of other related complex oxides, such as BaCoO_{3- δ} , Ba₂CoO₄, Pr₂BaCoO₅ etc., is known to date. Hence, to provide required thermodynamic calculations, one needs reasonable estimation of an entropy value. Regarding that, one can assume that the closest analogues have similar values of entropies. For this reason, 280 J·mol⁻¹·K⁻¹ as the value of standard entropy of NdBaCo₂O_{6- δ} [31] was employed as that of PBC. Aiming at obtaining at least approximate overview of phase stability under particular conditions rather than evaluating the exact phase diagrams, the other complex oxide phases (such as BaCoO_{3- δ} , Ba₂CoO₄, Pr₂BaCoO₅) were omitted in the calculations because of the absence of their thermodynamic

functions. The required thermodynamic data for corresponding simple oxides, carbonates and gaseous species (O_2 and CO_2) were taken from the FactPS database [29]. The thermodynamic calculations were carried out using Gibbs free energy minimization algorithm implemented in Maple software (MapleSoft, Waterloo, ON, Canada). The results are presented in Figures 1 and 2.

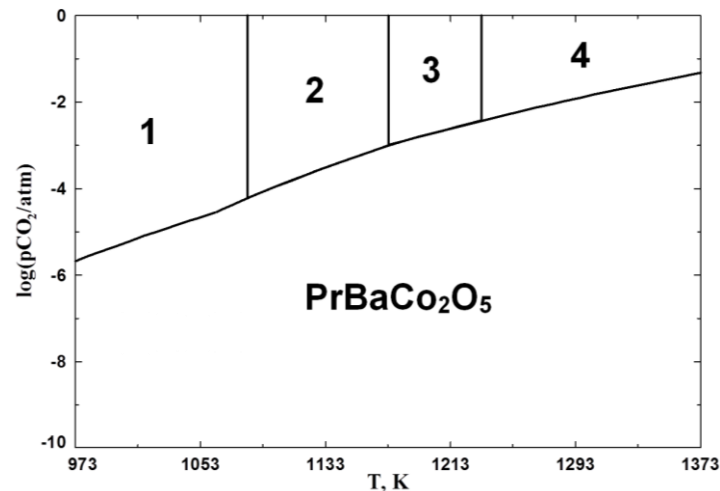


Figure 1. Equilibrium diagram calculated for $\text{PrBaCo}_2\text{O}_5\text{-CO}_2$ system at $p\text{O}_2 = 0.21$ atm. 1: $\text{BaCO}_3(\alpha\text{-phase}) + \text{PrCoO}_3 + \text{Co}_3\text{O}_4$; 2: $\text{BaCO}_3(\beta\text{-phase}) + \text{PrCoO}_3 + \text{Co}_3\text{O}_4$; 3: $\text{BaCO}_3(\beta\text{-phase}) + \text{PrCoO}_3 + \text{CoO}$; 4: $\text{BaCO}_3(\gamma\text{-phase}) + \text{PrCoO}_3 + \text{CoO}$.

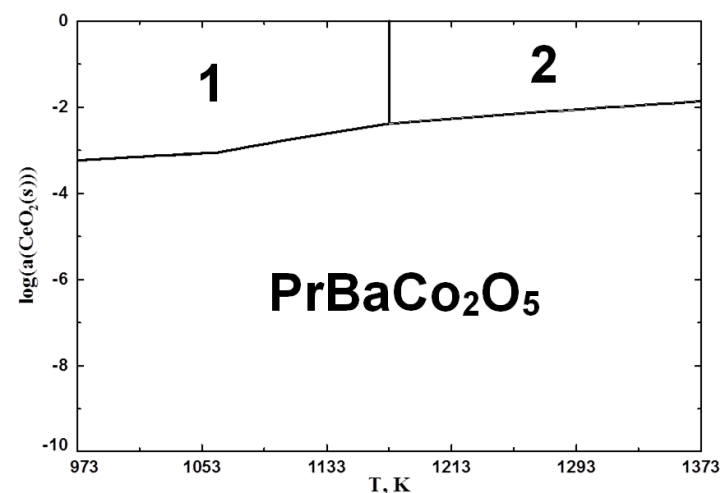


Figure 2. Equilibrium diagram calculated for $\text{PrBaCo}_2\text{O}_5\text{-CeO}_2$ system at $p\text{O}_2 = 0.21$ atm. 1: $\text{BaCeO}_3 + \text{PrCoO}_3 + \text{Co}_3\text{O}_4$; 2: $\text{BaCeO}_3 + \text{PrCoO}_3 + \text{CoO}$.

As seen in Figure 1, PBC is unstable in the atmosphere containing significant concentration of CO_2 and, moreover, its stability decreases with temperature. As a result, one can expect on the basis of the calculated diagram that PBC cathode should suffer from interaction with CO_2 from natural air (with 0.02–0.04 vol.% of CO_2 [32]) at temperatures less than ca. 1130 K. This prediction seems to coincide with the experimental results since formation of surface carbonates was often observed for double perovskites [10,22,33–35]. Therefore, interaction of double perovskites with CO_2 represents a significant challenge since IT-SOFCs usually operate in the temperature range 873–1073 K. Therefore, to maintain the long-term stability of the PBC cathode in CO_2 -containing atmosphere, its composition should be modified by adding suitable dopant.

Figure 2, in turn, shows that PBC is unstable against the chemical interaction with CeO_2 and, therefore, the PBC cathode should suffer from interaction with ceria-based solid electrolytes as well.

Therefore, as it was assumed in the Introduction, controversial results [10–23] on chemical compatibility of PBC and ceria-based electrolyte should be due to the kinetic limitations of interaction in solid state. Moreover, it is quite expected that such a chemical reactivity will also affect the long-term efficiency of PBC-based cathodes in contact with ceria electrolytes. In order to verify experimentally the results of thermodynamic analysis and to understand the possible influence of chemical incompatibility of PBC and ceria on the cathode properties, the chemical interaction between them was studied in detail.

3.2. Experimental Verification of the Results of Thermodynamic Analysis

The XRD patterns of the PBC-SDC (50:50 wt.%) mixture calcined in the temperature range 1000–1200 °C for 12 h in air are shown in Figure 3. At a first glance, there seem to be no evidence of a chemical interaction between the components of the mixture since there is no indication for the presence of a third phase. All the diffraction peaks can be indexed based on a physical mixture of PBC and SDC. Nevertheless, detailed analysis of the XRD patterns reveals a systematic shift of all the diffraction peaks. As a result, the refined lattice parameters of the PBC and SDC given in Figure 4 also show a noticeable change with calcination temperature. As seen in Figure 4, the parameter a for PBC remains, in practical terms, unchanged during calcination in the mixture with SDC whereas parameters c and a for PBC and SDC, respectively, decrease with increasing calcination temperature. Possible explanation for the observed change of the cell parameters is interdiffusion or, in other words, redistribution of some cations between PBC and SDC phases. Analysis of the available literature [36] revealed that only Pr or Co dissolution in SDC can potentially lead to the observed decrease of SDC cell parameter. However, the solubility limit for Co oxide in ceria does not exceed 3 mol.% even at 1580 °C [37] whereas rare-earth oxides are highly soluble in CeO_2 [38,39]. Therefore, it looks quite reasonable to expect that Pr from PBC dissolves in the SDC lattice and thereby causes the decrease of its parameter. At the same time, it seems unlikely to find large Pr deficiency in PBC [40]. It gives rise to assumption that Sm cations from SDC simultaneously occupy vacant sites in Pr-sublattice of PBC and, thereby, prevent its decomposition. However, Ce is the only rare-earth element which does not form double perovskites of the $\text{RBaCo}_2\text{O}_{6-\delta}$ -type and, therefore, dissolution of Ce in PBC lattice seems to be doubtful.

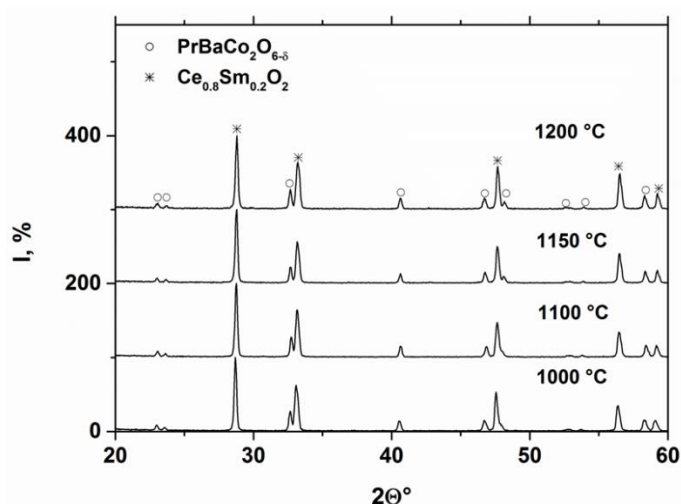


Figure 3. The XRD patterns of $\text{PrBaCo}_2\text{O}_{6-\delta}$ - $\text{Ce}_{0.8}\text{Sm}_{0.2}\text{O}_{1.9}$ (50:50 wt.%) mixtures calcined at different temperatures for 12 h in air.

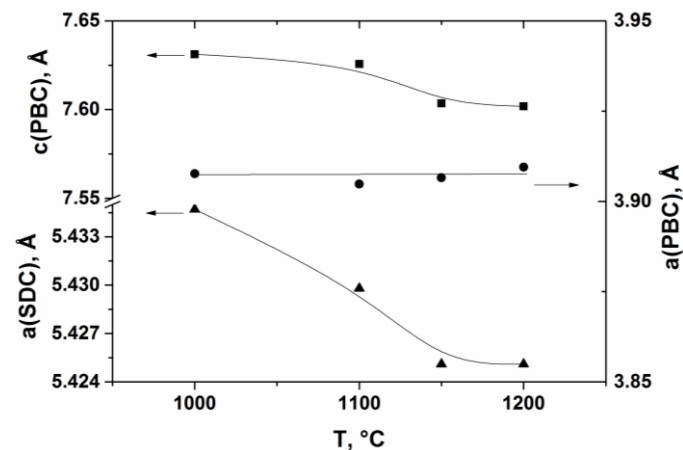


Figure 4. PBC and SDC cell parameter versus calcination (for 12 h in air) temperature. Lines are guide to eye only.

In order to reveal whether the cation interdiffusion is the case for PBC and SDC, appropriate diffusion couple was prepared and annealed at 1000 °C for 30 h in air. The SEM micrograph of the cross-section of this diffusion couple and element maps are shown in Figure 5.

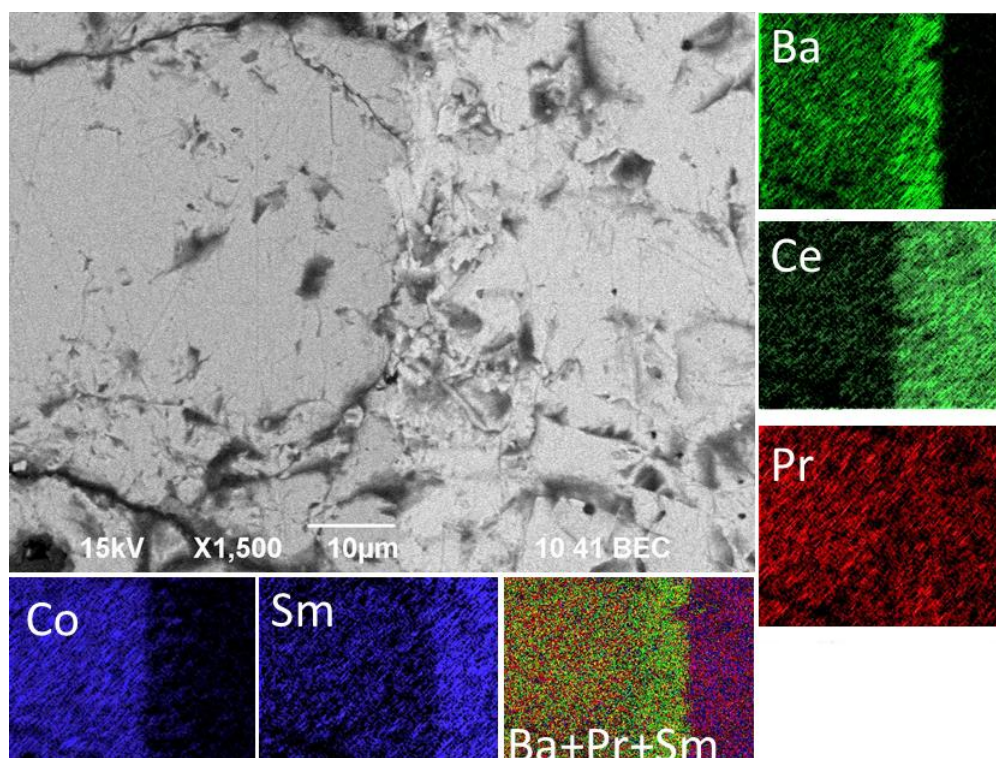


Figure 5. SEM micrograph of the cross-section of the PBC-SDC diffusion couple annealed at 1000 °C for 30 h in air and element maps.

As seen in Figure 5, strong diffusion of Pr into the SDC phase is indeed coupled with some diffusion of Sm into the PBC phase. At the same time, distribution of Co is mostly restricted by the PBC phase in agreement with low solubility of cobalt in doped ceria [37] whereas Ce is mostly distributed over the SDC phase. Furthermore, Figure 5 shows obvious evidence of Ba accumulation on the border between the PBC and SDC phases and formation of the intermediate layer (about 10 μm thick) with composition close to $\text{BaCe}_{1-x}\text{Pr}_x\text{O}_{3-\delta}$ with $x \approx 0.1\text{--}0.2$. This result reveals the chemical interaction

between PBC and SDC in full agreement with the prediction based on the thermodynamic calculations mentioned above.

Using XRD alone, it should be almost impossible to detect the $\text{BaCe}_{1-x}\text{Pr}_x\text{O}_{3-\delta}$ formation in PBC-SDC mixture, because the highest-intensity peak of SDC almost coincides with that of $\text{BaCe}_{1-x}\text{Pr}_x\text{O}_{3-\delta}$, effectively masking the latter [41]. In this respect, one can emphasize the key importance of knowledge of the standard thermodynamic functions of formation for the advanced materials since this enables prediction of chemical compatibility of such materials in easy way. Unfortunately, it is worth noting that conclusions on the stability of materials under operating conditions are very often made only on the basis of costly and time-consuming trial and error method without any thermodynamic calculations, which leads to the contradictory results obtained by different authors [10–22]. Thereby the importance and predictive power of thermodynamics, noticed by Albert Einstein [42], are still actual in the field of the material sciences.

3.3. The Effect of Cation Interdiffusion and Chemical Reactivity on The Properties of PBC–SDC Composites

Now, it is of great interest to understand whether the cation redistribution and chemical interaction of PBC and SDC discussed above are unfavorable for the efficiency of the PBC-SDC composite cathodes or not. First of all, available literature data [43] show that dissolution of Pr in SDC significantly increases thermal expansion coefficient (TEC) of the latter. Indeed, TEC of $\text{Ce}_{0.8}\text{Sm}_{0.2}\text{O}_{2-\delta}$ was found to be 12.3×10^{-6} – $12.9 \times 10^{-6} \text{ K}^{-1}$ [44,45] whereas that of $\text{Ce}_{0.8}\text{Pr}_{0.2}\text{O}_{2-\delta}$ is considerably higher and reaches $19 \times 10^{-6} \text{ K}^{-1}$ [43]. Dissolution of Sm in PBC, on the contrary, influences its TEC only a bit [12]. Therefore, pronounced interdiffusion of Pr and Sm between PBC and SDC in the composite should lead to the increase of the thermal expansion of ceria. As a result, TEC of the composite material is expected to change insignificantly (upon addition of the electrolyte phase) remaining very close to that of the double perovskite phase. Therefore, employment of the PBC-SDC composite instead of the PBC single phase seems to be not the right way to eliminate the mismatch in TEC between the cathode and electrolyte materials. The measured thermal expansion of the PBC-SDC composites along with that of PBC and SDC is given in Figure 6 and Table 1. For the sake of comparison, available literature data are also provided in the latter. As seen in Figure 6, the behavior of the thermal expansion predicted above coincides completely with that experimentally observed.

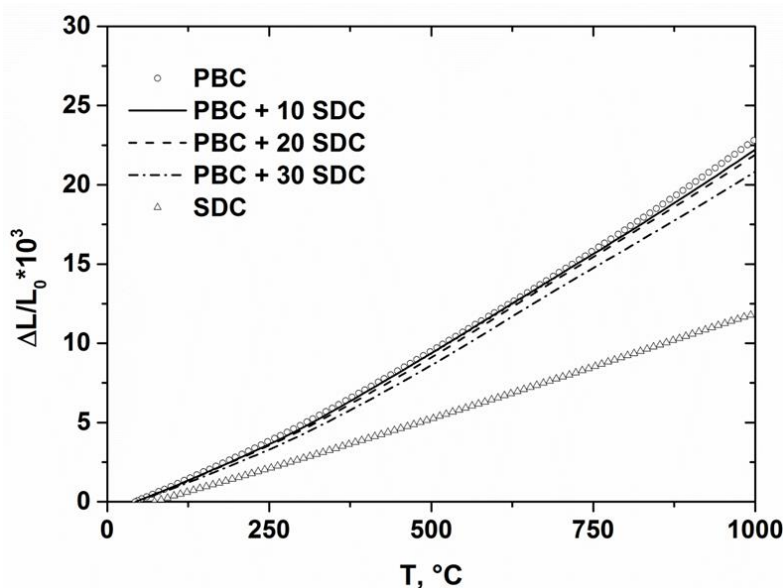


Figure 6. Thermal expansion of $(100 - y)\text{PBC}-y\text{SDC}$ ($y = 0$ – 30 wt.%) cathode materials and $\text{Ce}_{0.8}\text{Sm}_{0.2}\text{O}_{1.9}$ electrolyte in air [45].

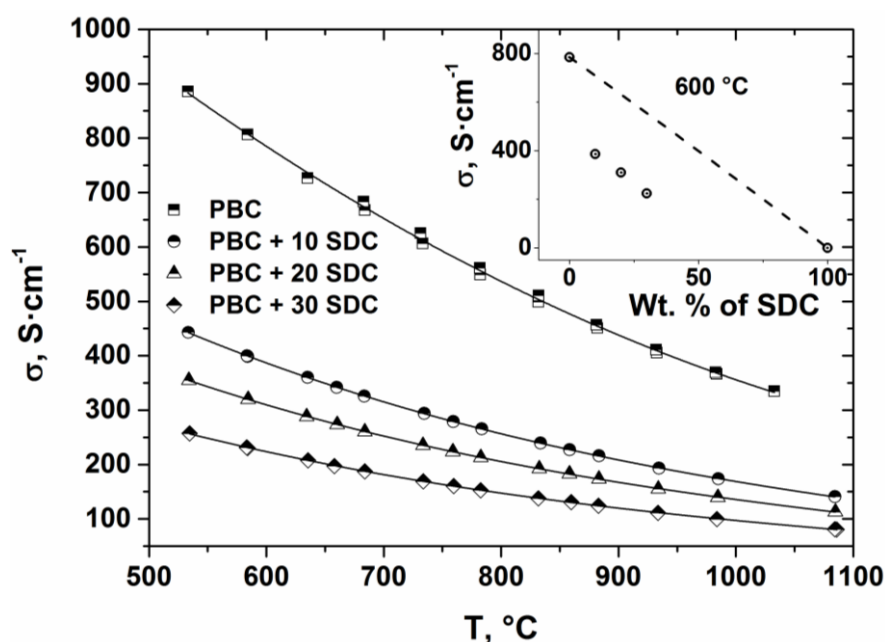
Table 1. The average TEC values of SDC electrolyte and $(100 - y)\text{PBC}-y\text{SDC}$ ($y = 0\text{--}30$ wt.%) cathode materials in the temperature range $30\text{--}1000$ °C in air.

Material	TEC · 10 ⁶ , K ^{−1}	
	This Work	References
PBC	24.6	23.8 [11], 24.1 [19]
90PBC-10SDC	24.1	-
80PBC-20SDC	23.8	21.3 [11]
70PBC-30SDC	22.8	-
SDC	12.9	12.3 [44]

As it follows from the Table 1, the measured TEC values are in good agreement with those reported in literature [11,19], and increasing SDC weight fraction leads to only little decrease of TEC of the composite. Therefore, mixing PBC with SDC does not improve thermal expansion behavior of the cathode material.

On the one hand, there seems to be a possibility to apply the single-phase PBC cathode on the surface of the SDC electrolyte without creating composites. Indeed, one can expect that cation redistribution will provide a transition layer with gradually decreasing TEC from that of PBC to the one of SDC. This transition layer is expected to have good adherence to both PBC and SDC and, consequently, might eliminate the TEC mismatch between them.

On the other hand, the expected drawback of Pr dissolution in SDC is to be an increase of the parasitic electronic conduction in the electrolyte whereas Sm dissolution in PBC can lead to somewhat decrease of its total conductivity [38]. Moreover, formation of BaCeO_3 interlayer on the PBC-SDC border as a result of the chemical interaction might cause increasing interfacial resistance. This will be also detrimental for the long-term stability of the SOFC cell performance since solid state chemical interaction, albeit proceeding slowly at moderate temperatures, will eventually lead to the formation of significant amount of the poorly-conducting phase on the interface during prolonged SOFC operation. Aforementioned assumptions are completely supported by the results of the PBC-SDC composites' total conductivity measurements given in Figure 7.

**Figure 7.** Temperature dependences of total conductivity of $(100 - y)\text{PBC}-y\text{SDC}$ ($y = 0\text{--}30$ wt.%) in air. The inset shows variation of the total conductivity of the composite with SDC content at 600 °C in air. Dashed line represents the weighted sum of PBC and SDC conductivity.

Pronounced drop in the electrical conductivity of the composite cathode material with increasing SDC content is obviously seen in Figure 7. Similar result was also reported in Reference [11]. Generally, this tendency is quite expected, taking into account that SDC has total conductivity that is lower than such of PBC on several orders of magnitude [46]. However, as seen in the inset of Figure 7, the drop in the conductivity is much larger than one would expect for a mechanical mixture of highly-conducting and poorly-conducting materials. Moreover, addition of only 10 wt.% of SDC causes abrupt (almost two times) drop in the conductivity. Further increase of SDC amount in the composite influences the conductivity to much less extent. This finding is quite consistent with the formation of the low-conducting BaCeO_3 layer on the boundary between PBC and SDC grains in the composite as discussed above. Therefore, the observed chemical interaction of PBC and SDC along with cation interdiffusion seems to seriously restrict the application of PBC as cathode material for SOFCs with doped ceria electrolyte. Taking into account that thermodynamic properties of A-site ordered double perovskite cobaltites are expected to be similar, the same restrictions should apply to them as well. However, one can expect that proton-conducting doped barium cerates and zirconates are more suitable electrolytes for application with such cathodes since they are believed to be thermodynamically stable against chemical interaction with the double perovskite cobaltites. These conclusions are consistent with experimental observation of phase stability of PBC in contact with BaCeO_3 -based electrolyte [47,48]. No new phase formation was found on the interface between them [47], but, as evidenced from the results of diffusion couple experiments (see Figure 5), Pr may diffuse into the BaCeO_3 -based electrolyte and most probably into BaZrO_3 -based electrolyte as well. The “outgoing” diffusion of Pr from PBC into BaCeO_3 or BaZrO_3 -based electrolyte in that case would be balanced by “incoming” flux of the dopant cation from the electrolyte to PBC. Some signs of such interdiffusion were observed in Reference [47]. It is obvious that Pr diffusion into the proton-conducting electrolyte would suppress its performance because of increasing electronic conductivity. Therefore, it would be better to use double perovskites containing other rare-earth elements instead of Pr. In addition, it is interesting to note that triple (proton, electron and oxide ion) conduction was found in some (Pr-free) double perovskites [49]. Taking into account all the circumstances mentioned above, it seems that these materials can be considered as particularly suitable for proton-conducting solid oxide fuel cells.

4. Conclusions

The thermodynamic analysis of the stability of PBC double perovskite under different conditions was carried out. As a result, its instability against chemical interaction with CO_2 and CeO_2 was revealed. In the latter case, diffusion couple (PBC-SDC) experiment showed interdiffusion of Pr and Sm and chemical interaction between PBC and SDC with formation of barium cerate as a product, in full agreement with thermodynamic calculations. This was shown to affect significantly both thermal expansion and total conductivity of the composites and lead to higher than expected TECs of the composites. Formation of barium cerate on the border between PBC and SDC was also shown to cause a significant drop in the composites’ total conductivity and should be detrimental for the long-term stability of the SOFC cell. One can expect that predicted on the basis of thermodynamic calculations formation of BaCO_3 due to the chemical reaction of PBC with CO_2 from the ambient air will lead to lowering of the SOFC performance as well. The PBC double perovskite was shown to be more suitable as electrode for proton-conducting solid oxide fuel cells because of its thermodynamic stability against chemical interaction with barium cerate- and zirconate-based electrolytes. However, in this case the interaction of PBC with CO_2 is still an issue.

Author Contributions: Conceptualization, D.T. and A.Z.; methodology, D.T. and A.Z.; investigation, N.T., I.I., D.M. and V.S.; writing—original draft preparation, D.T., D.M. and A.Z.; supervision, A.Z.

Funding: Tsvetkova acknowledges the financial support of the Russian Foundation for Basic Research (grant No. 16-33-00188). Dmitry Tsvetkov, Ivan Ivanov, Dmitry Malyshev, Vladimir Sereda and Andrey Zuev are grateful to the Ministry of Education and Science of Russian Federation (State Task No. 4.2288.2017/PCh).

Conflicts of Interest: The authors declare no conflict of interest. The funders had no role in the design of the study; in the collection, analyses, or interpretation of data; in the writing of the manuscript, or in the decision to publish the results.

References

1. Anjum, U.; Vashishtha, S.; Agarwal, M.; Tiwari, P.; Sinha, N.; Agrawal, A.; Basu, S.; Haider, M.A. Oxygen anion diffusion in double perovskite $\text{GdBaCo}_2\text{O}_{5+\delta}$ and $\text{LnBa}_{0.5}\text{Sr}_{0.5}\text{Co}_{2-x}\text{Fe}_x\text{O}_{5+\delta}$ (Ln = Gd, Pr, Nd) electrodes. *Int. J. Hydrog. Energy* **2016**, *41*, 7631–7640. [\[CrossRef\]](#)
2. Li, S.; Xia, T.; Li, Q.; Sun, L.; Huo, L.; Zhao, H. A-site Ba-deficiency layered perovskite $\text{EuBa}_{1-x}\text{Co}_2\text{O}_{6-\delta}$ cathodes for intermediate-temperature solid oxide fuel cells: Electrochemical properties and oxygen reduction reaction kinetics. *Int. J. Hydrog. Energy* **2017**, *42*, 24412–24425. [\[CrossRef\]](#)
3. Yi, K.; Sun, L.; Li, Q.; Xia, T.; Huo, L.; Zhao, H.; Li, J.; Lü, Z.; Bassat, J.-M.; Rougier, A.; et al. Effect of Nd-deficiency on electrochemical properties of $\text{NdBaCo}_2\text{O}_{6-\delta}$ cathode for intermediate-temperature solid oxide fuel cells. *Int. J. Hydrog. Energy* **2016**, *41*, 10228–10238. [\[CrossRef\]](#)
4. Pang, S.; Wang, W.; Chen, T.; Wang, Y.; Xu, K.; Shen, X.; Xi, X.; Fan, J. The effect of potassium on the properties of $\text{PrBa}_{1-x}\text{Co}_2\text{O}_{5+\delta}$ ($x = 0.00\text{--}0.10$) cathodes for intermediate-temperature solid oxide fuel cells. *Int. J. Hydrog. Energy* **2016**, *41*, 13705–13714. [\[CrossRef\]](#)
5. Subardi, A.; Chen, C.-C.; Fu, Y.-P. Oxygen transportation, electrical conductivity and electrochemical properties of layered perovskite $\text{SmBa}_{0.5}\text{Sr}_{0.5}\text{Co}_2\text{O}_{5+\delta}$. *Int. J. Hydrog. Energy* **2017**, *42*, 5284–5294. [\[CrossRef\]](#)
6. Zhang, L.; Li, S.; Xia, T.; Sun, L.; Huo, L.; Zhao, H. Co-deficient $\text{PrBaCo}_{2-x}\text{O}_{6-\delta}$ perovskites as cathode materials for intermediate-temperature solid oxide fuel cells: Enhanced electrochemical performance and oxygen reduction kinetics. *Int. J. Hydrog. Energy* **2018**, *43*, 3761–3775. [\[CrossRef\]](#)
7. Huang, X.; Feng, J.; Abdellatif, H.R.S.; Zou, J.; Zhang, G.; Ni, C. Electrochemical evaluation of double perovskite $\text{PrBaCo}_{2-x}\text{Mn}_x\text{O}_{5+\delta}$ ($x = 0, 0.5, 1$) as promising cathodes for IT-SOFCs. *Int. J. Hydrog. Energy* **2018**, *43*, 8962–8971. [\[CrossRef\]](#)
8. Zhang, K.; Ge, L.; Ran, R.; Shao, Z.; Liu, S. Synthesis, characterization and evaluation of cation-ordered $\text{LnBaCo}_2\text{O}_{5+\delta}$ as materials of oxygen permeation membranes and cathodes of SOFCs. *Acta Mater.* **2008**, *56*, 4876–4889. [\[CrossRef\]](#)
9. Li, N.; Lü, Z.; Wei, B.; Huang, X.; Chen, K.; Zhang, Y.; Su, W. Characterization of $\text{GdBaCo}_2\text{O}_{5+\delta}$ cathode for IT-SOFCs. *J. Alloys Compd.* **2008**, *454*, 274–279. [\[CrossRef\]](#)
10. Tarancón, A.; Peña-Martínez, J.; Marrero-López, D.; Morata, A.; Ruiz-Morales, J.C.; Núñez, P. Stability, chemical compatibility and electrochemical performance of $\text{GdBaCo}_2\text{O}_{5+x}$ layered perovskite as a cathode for intermediate temperature solid oxide fuel cells. *Solid State Ion.* **2008**, *179*, 2372–2378. [\[CrossRef\]](#)
11. Chen, D.; Ran, R.; Shao, Z. Assessment of $\text{PrBaCo}_2\text{O}_{5+\delta} + \text{Sm}_{0.2}\text{Ce}_{0.8}\text{O}_{1.9}$ composites prepared by physical mixing as electrodes of solid oxide fuel cells. *J. Power Sources* **2010**, *195*, 7187–7195. [\[CrossRef\]](#)
12. Kim, J.H.; Kim, Y.; Connor, P.A.; Irvine, J.T.S.; Bae, J.; Zhou, W. Structural, thermal and electrochemical properties of layered perovskite $\text{SmBaCo}_2\text{O}_{5+\delta}$, a potential cathode material for intermediate-temperature solid oxide fuel cells. *J. Power Sources* **2009**, *194*, 704–711. [\[CrossRef\]](#)
13. Zhao, L.; He, B.; Xun, Z.; Wang, H.; Peng, R.; Meng, G.; Liu, X. Characterization and evaluation of $\text{NdBaCo}_2\text{O}_{5+\delta}$ cathode for proton-conducting solid oxide fuel cells. *Int. J. Hydrog. Energy* **2010**, *35*, 753–756. [\[CrossRef\]](#)
14. Kim, G.; Wang, S.; Jacobson, A.J.; Reimus, L.; Brodersen, P.; Mims, C.A. Rapid oxygen ion diffusion and surface exchange kinetics in $\text{PrBaCo}_2\text{O}_{5+x}$ with a perovskite related structure and ordered A cations. *J. Mater. Chem.* **2007**, *17*, 2500–2505. [\[CrossRef\]](#)
15. Frison, R.; Portier, S.; Martin, M.; Conder, K. Study of oxygen tracer diffusion in $\text{PrBaCo}_2\text{O}_{5.74}$ by SIMS. *Nucl. Instrum. Methods Phys. Res. Sect. B* **2012**, *273*, 142–145. [\[CrossRef\]](#)
16. Yoo, C.-Y.; Boukamp, B.A.; Bouwmeester, H.J.M. Oxygen surface exchange kinetics on $\text{PrBaCo}_2\text{O}_{5+\delta}$. *Solid State Ion.* **2014**, *262*, 668–671. [\[CrossRef\]](#)
17. Zhao, L.; He, B.; Lin, B.; Ding, H.; Wang, S.; Ling, Y.; Peng, R.; Meng, G.; Liu, X. High performance of proton-conducting solid oxide fuel cell with a layered $\text{PrBaCo}_2\text{O}_{5+\delta}$ cathode. *J. Power Sources* **2009**, *194*, 835–837. [\[CrossRef\]](#)

18. Zhou, Q.; Wang, F.; Shen, Y.; He, T. Performances of $\text{LnBaCo}_2\text{O}_{5+x}\text{--Ce}_{0.8}\text{Sm}_{0.2}\text{O}_{1.9}$ composite cathodes for intermediate-temperature solid oxide fuel cells. *J. Power Sources* **2010**, *195*, 2174–2181. [CrossRef]
19. Zhao, L.; Nian, Q.; He, B.; Lin, B.; Ding, H.; Wang, S.; Peng, R.; Meng, G.; Liu, X. Novel layered perovskite oxide $\text{PrBaCuCoO}_{5+\delta}$ as a potential cathode for intermediate-temperature solid oxide fuel cells. *J. Power Sources* **2010**, *195*, 453–456. [CrossRef]
20. Zhu, C.; Liu, X.; Yi, C.; Pei, L.; Wang, D.; Yan, D.; Yao, K.; Lü, T.; Su, W. High-performance $\text{PrBaCo}_2\text{O}_{5+\delta}\text{--Ce}_{0.8}\text{Sm}_{0.2}\text{O}_{1.9}$ composite cathodes for intermediate temperature solid oxide fuel cell. *J. Power Sources* **2010**, *195*, 3504–3507. [CrossRef]
21. Chen, D.; Ran, R.; Zhang, K.; Wang, J.; Shao, Z. Intermediate-temperature electrochemical performance of a polycrystalline $\text{PrBaCo}_2\text{O}_{5+\delta}$ cathode on samarium-doped ceria electrolyte. *J. Power Sources* **2009**, *188*, 96–105. [CrossRef]
22. Pelosato, R.; Cordaro, G.; Stucchi, D.; Cristiani, C.; Dotelli, G. Cobalt based layered perovskites as cathode material for intermediate temperature Solid Oxide Fuel Cells: A brief review. *J. Power Sources* **2015**, *298*, 46–67. [CrossRef]
23. Choi, S.; Park, S.; Shin, J.; Kim, G. The effect of calcium doping on the improvement of performance and durability in a layered perovskite cathode for intermediate-temperature solid oxide fuel cells. *J. Mater. Chem. A* **2015**, *3*, 6088–6095. [CrossRef]
24. Ivanov, I.L.; Malyshev, D.A.; Tsvetkova, N.S.; Sereda, V.V.; Kiselev, E.A.; Zuev, A.Y.; Tsvetkov, D.S. Oxygen content and thermodynamics of formation of double perovskites $\text{REBaCo}_2\text{O}_{6-\delta}$ (RE = Gd, Pr). *Thermochim. Acta* **2014**, *578*, 28–32. [CrossRef]
25. Cordfunke, E.H.P.; Booi, A.S.; Huntelaar, M.E. The thermochemical properties of $\text{BaCeO}_3(\text{s})$ and $\text{SrCeO}_3(\text{s})$ from $T = (5 \text{ to } 1500) \text{ K}$. *J. Chem. Thermodyn.* **1998**, *30*, 437–447. [CrossRef]
26. Sahu, S.K.; Tanasescu, S.; Scherrer, B.; Marinescu, C.; Navrotsky, A. Energetics of lanthanide cobalt perovskites: $\text{LnCoO}_{3-\delta}$ (Ln = La, Nd, Sm, Gd). *J. Mater. Chem. A* **2015**, *3*, 19490–19496. [CrossRef]
27. Petrov, A.N.; Cherepanov, V.A.; Zuyev, A.Yu.; Zhukovsky, V.M. Thermodynamic stability of ternary oxides in Ln-M-O (Ln = La, Pr, Nd; M = Co, Ni, Cu) systems. *J. Solid State Chem.* **1988**, *77*, 1–14. [CrossRef]
28. Tsubouchi, S.; Kyômen, T.; Itoh, M.; Oguni, M. Electric, magnetic, and calorimetric properties and phase diagram of $\text{Pr}_{1-x}\text{Ca}_x\text{CoO}_3$ ($0 < x < 0.55$). *Phys. Rev. B* **2004**, *69*, 144406. [CrossRef]
29. Fact-Web Suite of Interactive Programs. Available online: www.factsage.com (accessed on 25 December 2018).
30. Petrov, A.N.; Zuev, A.Y.; Vylkov, A.I. Thermodynamics of point defects and mechanism of charge transfer in copper-containing lanthanum cobaltite $\text{LaCo}_{1-x}\text{Cu}_x\text{O}_{3-\delta}$ ($x = 0.3$). *Russ. J. Phys. Chem. A* **2005**, *79*, 220–225.
31. Tsvetkov, D.S.; Sereda, V.V.; Malyshev, D.A.; Druzhinina, A.I.; Zuev, A.Y. Thermodynamics of formation of double perovskite $\text{NdBaCo}_2\text{O}_{6-\delta}$. *J. Chem. Thermodyn.* under review.
32. WMO Greenhouse Gas Bulletin No. 12. Available online: <https://public.wmo.int> (accessed on 25 December 2018).
33. Kim, J.P.; Pyo, D.W.; Magnone, E.; Park, J.H. Preparation and Oxygen Permeability of $\text{ReBaCo}_2\text{O}_{5+\delta}$ (Re = Pr, Nd, Y) Ceramic Membranes. *Adv. Mater. Res.* **2012**, *560*, 959–964. [CrossRef]
34. Arulmozhi, N.; Kan, W.H.; Thangadurai, V.; Karan, K. Kinetics and thermodynamics of carbonation of a promising SOFC cathode material $\text{La}_{0.5}\text{Ba}_{0.5}\text{CoO}_{3-\delta}$ (LBC). *J. Mater. Chem. A* **2013**, *1*, 15117–15127. [CrossRef]
35. Zhu, L.; Wei, B.; Lü, Z.; Feng, J.; Xu, L.; Gao, H.; Zhang, Y.; Huang, X. Performance degradation of double-perovskite $\text{PrBaCo}_2\text{O}_{5+\delta}$ oxygen electrode in CO_2 containing atmospheres. *Appl. Surf. Sci.* **2017**, *416*, 649–655. [CrossRef]
36. Kim, D.-J. Lattice Parameters, Ionic Conductivities, and Solubility Limits in Fluorite-Structure MO_2 Oxide [$\text{M} = \text{Hf}^{4+}, \text{Zr}^{4+}, \text{Ce}^{4+}, \text{Th}^{4+}, \text{U}^{4+}$] Solid Solutions. *J. Am. Ceram. Soc.* **1989**, *72*, 1415–1421. [CrossRef]
37. Chen, M.; Hallstedt, B.; Grundy, A.N.; Gauckler, L.J. $\text{CeO}_2\text{--CoO}$ Phase Diagram. *J. Am. Ceram. Soc.* **2004**, *86*, 1567–1570. [CrossRef]
38. Etsell, T.H.; Flengas, S.N. Electrical properties of solid oxide electrolytes. *Chem. Rev.* **1970**, *70*, 339–376. [CrossRef]
39. Bevan, D.J.M.; Summerville, E. Chapter 28 Mixed rare earth oxides. In *Handbook on the Physics and Chemistry of Rare Earths*; Gschneider, K.A., Eyring, L., Eds.; Elsevier: North Holland, Amsterdam, The Netherlands, 1979; Volume 3, pp. 401–524.

40. Jiang, X.; Shi, Y.; Zhou, W.; Li, X.; Su, Z.; Pang, S.; Jiang, L. Effects of Pr^{3+} -deficiency on structure and properties of $\text{PrBaCo}_2\text{O}_{5+\delta}$ cathode material—A comparison with Ba^{2+} -deficiency case. *J. Power Sources* **2014**, *272*, 371–377. [[CrossRef](#)]
41. Basbus, J.F.; Caneiro, A.; Suescun, L.; Lamas, D.G.; Mogni, L.V. Anomalous X-ray diffraction study of Pr-substituted $\text{BaCeO}_{3-\delta}$. *Acta Crystallogr. Sect. B* **2015**, *71*, 455–462. [[CrossRef](#)]
42. Einstein, A. *Autobiographical Notes in The Library of Living Philosophers*, V.VII.; Open Court Publishing Company: La Salle, IL, USA, 1973; p. 33.
43. Kuru, Y.; Bishop, S.R.; Kim, J.J.; Yildiz, B.; Tuller, H.L. Chemomechanical properties and microstructural stability of nanocrystalline Pr-doped ceria: An in situ X-ray diffraction investigation. *Solid State Ion.* **2011**, *193*, 1–4. [[CrossRef](#)]
44. Pikalova, E.Y.; Maragou, V.I.; Demina, A.N.; Demin, A.K.; Tsiakaras, P.E. The effect of co-dopant addition on the properties of $\text{Ln}_{0.2}\text{Ce}_{0.8}\text{O}_{2-\delta}$ ($\text{Ln}=\text{Gd}, \text{Sm}, \text{La}$) solid-state electrolyte. *J. Power Sources* **2008**, *181*, 199–206. [[CrossRef](#)]
45. Tsvetkova, N.S.; Zuev, A.Y.; Tsvetkov, D.S. Investigation of $\text{GdBaCo}_{2-x}\text{Fe}_x\text{O}_{6-\delta}$ ($x = 0, 0.2$)— $\text{Ce}_{0.8}\text{Sm}_{0.2}\text{O}_2$ composite cathodes for intermediate temperature solid oxide fuel cells. *J. Power Sources* **2013**, *243*, 403–408. [[CrossRef](#)]
46. Brett, D.J.L.; Atkinson, A.; Brandon, N.P.; Skinner, S.J. Intermediate temperature solid oxide fuel cells. *Chem. Soc. Rev.* **2008**, *37*, 1568–1578. [[CrossRef](#)]
47. Lin, Y.; Ran, R.; Zhang, C.; Cai, R.; Shao, Z. Performance of $\text{PrBaCo}_2\text{O}_{5+\delta}$ as a Proton-Conducting Solid-Oxide Fuel Cell Cathode. *J. Phys. Chem. A* **2010**, *114*, 3764–3772. [[CrossRef](#)]
48. Medvedev, D.A.; Lyagaeva, J.G.; Gorbova, E.V.; Demin, A.K.; Tsiakaras, P. Advanced materials for SOFC application: Strategies for the development of highly conductive and stable solid oxide proton electrolytes. *Prog. Mater. Sci.* **2016**, *75*, 38–79. [[CrossRef](#)]
49. Strandbakke, R.; Cherepanov, V.A.; Zuev, A.Y.; Tsvetkov, D.S.; Argirusis, C.; Sourkouni, G.; Prünke, S.; Norby, T. Gd- and Pr-based double perovskite cobaltites as oxygen electrodes for proton ceramic fuel cells and electrolyser cells. *Solid State Ion.* **2015**, *278*, 120–132. [[CrossRef](#)]



© 2019 by the authors. Licensee MDPI, Basel, Switzerland. This article is an open access article distributed under the terms and conditions of the Creative Commons Attribution (CC BY) license (<http://creativecommons.org/licenses/by/4.0/>).